CRACK INITIATION AND GROWTH IN WELDS AT 1100° F (593°C)

M. J. MANJOINE

Westinghouse Electric Corporation, Research and Development Center, 1310 Beulah Road, Pittsburgh, Pennsylvania 15235, U.S.A.

SUMMARY

Welds are often loaded under a high degree of plane strain. The crack initiation and crack growth at elevated temperature of a weldment under a high degree of plane strain was investigated. The weldment consisted of a central axial weld of type 308 stainless steel with controlled residual elements in a type 304 stainless steel plate. The length of the weldment was less than the width and the heads were reinforced to reduce the stress and to prevent lateral strain. Thus the degree of plane strain was highest at the heads and decreased toward mid-length. For this axial weld specimen, the weld metal, the heat affected zone (HAZ) and the base metal are all loaded in parallel so that the overall axial defections are the same. The life for the weld metal at the stresses employed in about eight times that of the base metal.

The purposes of the rupture tests performed at 1100 °F (593 °C) were to determine the strain for crack initiation and to study the factors which influence the crack growth rate.

The gradient of plane strain in the weldment causes the axial strain to be a minimum at the heads and to increase toward mid-length. This enables a study of the strain for crack initiation along the specimen length as the creep strains increase with time. The local strains along the length and in the various parts of the weldment were determined during the tests by measurements from photographs of a grid on the surface of the specimen.

It is postulated that the cracks initiate from an exhaustion of local ductility which is a function of the strain rate and stress state. In these tests it was found that intergranular cracks initiated along the HAZ of the weld at regular spacing when the local axial strain exceeded about 4% for the creep rate of about 4×10^{-5} per hour. The time at crack initiation is about equal to that for rupture of the base metal at the same average stress level. The general transverse direction of the crack growth is perpendicular to the direction of the maximum principal stress. The crack growth rate at each HAZ was proportional to the net section creep rate which also controls the crack-opening-displacement rates. The transverse crack growth rate is about six times faster in the base metal than that across the weld. Accelerated crack growth rate occurs when the cracks on each side of the weld grow sufficiently to interact.

Acknowledgment: This research was sponsored by the U.S. Energy Research and Development Administration Division of Reactor Research and Development under Contract No. E(11-1)3045.

1. Introduction

The deformation of welds in a component can be subject to a high directional restraint resulting from the geometry and loading. An example is a circumferential weld in a pipe or pressure vessel where the weld is often loaded with a high degree of plane strain since the longitudinal strain (transverse to the weld) is restricted. This paper describes the deformations, of a type 304 stainless steel plate with a central axial weld of type 308 stainless steel with controlled residual elements,under uniaxial creep loading at an average stress of 159 MPa. The local strain for crack initiation and the characteristics of creep crack growth were studied by taking continuous and periodic deformation measurements, as well as, photographs of the grid. The measurement techniques for the grid were previously described by the author [1].

Another purpose of the strain distribution measurements is their use in validation of elevated temperature analytical methods.

A high degree of plane strain was achieved over the gage section by: (a) lateral reinforcement at the heads, (b) ratio of width to thickness of ten, and (c) ratio of width to length of four. This geometry produces plane strain at the heads and the degree of plane strain diminishes gradually toward mid-length of the gauge section where the ratio of average axial strain to average lateral strain is about five. For the loading imposed the base plate material, the heat affected zones and the weld metal are strained in parallel.

2. Test Model and Instrumentation

The test model was formed by welding two plates of annealed type 304 stainless steel from reference heat 9T2796 with type 308 stainless steel weld metal with controlled residual elements. The weld metal has been characterized by King, et al. [2]. Plates of 12.7 mm thickness were separated with a gap of 12.7 mm which was filled with weld metal. The weldment was machined to a thickness of 8.5 mm and to a gage section of uniform width of 85 mm by 21 mm long. The axial weld was centered in the gage section. A radius of 8.5 mm joined the gage section to the 102 mm wide head, see Figs. 1 and 2. After finish machining, the weldment was prepared with a photo grid of 0.85 mm squares. Extension pieces 85 mm thick by 102 mm wide by 285 mm long were welded to each face of the test plate at each end to apply the axial load and reinforce the heads.

A photograph of the plate specimen with the central axial weld after 2886 hours at 159 MPa and 593°C, Fig. 1, shows the test section, dummy blocks between the fillets, extension plates, and instrumentation. The extension pieces were welded only at the edges of the test weldment and at the two symmetrical pockets with the nearest edge about 25 mm from the uniform gage section. Thus the extension plates restricted the lateral deformation but minimized any thickness restraint while applying a nearly uniform axial load to the gage section. The unloaded dummy blocks have the same photo grid as the test section and are used to obtain the scale factor for the photographs taken during the creep test. They can also be used to carry the dummy strain gauge for temperature compensation.

The instrumentation consists of nine thermocouples, three on both the top and bottom heads and one at top, middle, and bottom of one of the dummy blocks, Fig. 1b. The overall deformation was measured continuously at each edge through extension rods clamped to the heads and clip gages (CG_1 and CG_2) equipped with resistance strain gages, Fig. 2. In

addition, the average strain was measured at two positions by weldable resistance strain gages (see Fig. 1b and insert in Fig. 2).

3. Test Procedure

The test assembly was thermally cycled three times to test temperature to stabilize the weldable strain gages. The loading was applied in increments when the temperature had stabilized and the loading deflections recorded.

During constant load creep testing the overall extension of the clip gages, the reading of strain gages and the thermocouples were recorded daily. The model was unloaded and cooled periodically (usually at about a 400 hour interval) for photographic recording at room temperature of the grid deformation.

4. Test Results

4.1 Comparison of Strain Measurements up to 188 Hours

At the initial loading, the strain gages and clip gages indicate that the proportional limit of this composite of weld and base metal in parallel is 85.7 MPa. The plastic or inelastic strains at 159 MPa were 0.048% at the weld centerline (SG 22) and 0.077% for the base metal (SG 25). The inelastic overall deflections were 7.6 μm for clip gage CG1 and 32 μm) for clip gage CG2. The latter indicates an initial bending or misalignment of the extensometer parts which corrected itself after the yielding. The inelastic readings of these gages during the first 188 hours of creep testing are compared in Fig. 2 with the permanent strains measured from the grid at the end of this period.

The plastic flow and creep resistance of the weld is higher than that of the base metal [2] and this is reflected in the loading and creep strains recorded by the strain gages. Since the weld metal and base metal are in parallel and the heads are reinforced beyond the gage section, the overall deflections of each must be nearly the same across the heads.

A comparison of the other strain gage measurements during the first 188 hours is also presented in Fig. 2. The clip gages measure over a longer gage length than that of the weldable strain gages. The deflections measured by the clip gages were, therefore, divided by 33 mm to obtain a "comparable" strain. The grid measurements and strain calculations were made for the same gauge length as that of the weldable strain gages, 29.2 mm.

Both weldable strain gages started to fail after about 0.7% inelastic strain or about 0.82% total strain. The strain at the centerline of the weld, SG 22, is less than that in the base metal, SG 25, and its creep rate is about the same as that from the clip gages, Fig. 2. An extrapolation of SG 22 to 188 hours is nearly the same as that obtained from the grid measurements. The grid measurement at 188 hours for the same location in the base metal as SG 25, A in Fig. 2, is about 0.12% strain higher than that at the centerline of the weld. Although the strains from clip gage 2 are slightly higher than those from CG1, the creep curves become parallel after about 40 hours. It is concluded that the initial bending or misalignment of the extensometer rods is corrected by the inelastic strains during this early period.

4.2 Axial Strain Distributions at the Centerline of the Weld

From the photographs of the grid taken at 188 hours and at about 400 hour intervals up to fracture, strain measurements were made along the axial centerline of the welds for every 5 divisions of the grid. The axial strain distributions at the center of the weld are illustrated in Fig. 3 for the given creep times. The axial strain is practically zero at the reinforced head where the area is four times that of the uniform section. The strain increases toward mid-length of the uniform section as the constraint of the head diminishes. With increasing creep time the strain increases for positions along the reduced section. The strain gradient also increases as the effect of the constraint increases with inelastic straining.

The extent of cracking in the heat effected zone is indicated on the curves and this data will be discussed later.

The peak strains from the grid measurements, open circles in Fig. 4, are plotted as a function of creep time. The average of the overall creep deflections from the clip gages has been converted to strain assuming gage length of 25.4 mm which gives a strain comparable to the maximum at the centerline of the weld. These data give a continuous curve and the trend can be compared with the maximum strains measured from the grid, Fig. 4. It can be seen that the agreement is good, the deviation over most of the curve is less than about 1/2% strain.

4.3 Axial Strain Profiles

The axial strain also varies across the width of the reduced section as well as along the length. Since the specimen is symmetrical about the mid-length of the reduced section, the readings from the grid are averaged for similar positions at each end and are plotted in Fig. 5 for the time of 1782 hours. At this time the overall creep rate is still at its minimum for the constant loading but is approaching the instability of the third stage of creep or the increasing creep rate region.

Near the heads, positions 1 and 9 in Fig. 5a, the strains are lowest and increase slightly from each side to the centerline. Near the fillets, positions 2 and 8, the strains are highest at the fillets and decrease toward the center. At positions 3 and 7 in the uniform width section, the strain is high at the edges near the fillets and decreases toward the heat affected zone, HAZ, with a local maximum at the center of the weld. Cracking has initiated at the HAZ. For positions 4-6 the strain is nearly uniform across the width. The strain at the left HAZ, Fig. 5a, is higher than that at the right because of a large crack at the left, Fig. 1a. At mid-length, position 5, the strain increases from the edges to the weld. Since a larger crack is at the right HAZ, Fig. 1a, the measured strain is higher than on the left side.

The axial strain as averaged across the width at a given axial length position is given in Fig. 5b. The axial permanent strains are essentially zero at the reinforced heads, increase nearly linearly toward mid-length and have two local maximums at the central cracks. The average strain is $5.6 \pm 0.4\%$ for the middle half of the uniform section length.

At 2886 hours (near rupture), Fig. 4, long cracks are present near the heat affected zones, Fig. 1, so that the strain profiles are becoming distorted near the weld. The lateral strains were measured for each 5 grid divisions across the width at five length positions

as shown in Fig. 6. Near the heads where the lateral constraint is a maximum, the lateral strain (curve a Fig. 6-1) is negative and the magnitude decreases from the edges to the centerline and the average strain across the width only -0.15%, Fig. 6-2. Near the middle of the fillet, curve e Fig. 6-1, the strains also decrease in magnitude from the edge to the centerline and the average is only -0.65%, Fig. 6-2. At the end of the uniform width near the fillet, curve b Fig. 6-1, the strains are about -3% at the edges and decrease in magnitude to about -1/2% at the centerline.

Near mid-length where the cracks are long, the strain profiles, curves c and d Fig. 6-1, show that the lateral strains decrease to a minimum at the heat affected zone, with a local maximum at the center of the weld. The averages of the lateral strain across the width, Fig. 6-2, is practically zero at the reinforced heads and increases in magnitude toward mid-length to a peak of about -2.5%.

For comparison the axial strains were measured for seven width positions at the same time of 2886 hours, Fig. 7. The discontinuities shown at the heat affected zones show large variation since some measurements are made across cracks. The axial strain profiles are averaged for similar length positions from each head. Near the fillets, curves 2-8 and 3-7 Fig. 7a, the axial strains are highest at the edges because of the strain concentration of the geometry and decrease for positions toward the centerline. Near mid-length the axial strain increases from the edges to a maximum at the center, curves 4-6 and 5 Fig. 7a. The average strains across the width, Fig. 7b, show the steep increase from the heads to mid-length and the similar behavior for each end.

4.4 Crack Initiation and Growth

In Fig. 1a five major cracks are evident. From the grid the axial location of each crack can be recorded and by checking at these locations in photographs taken earlier in life, the initiation and growth can be followed. The first surface crack to be visible in the photographs is the upper one to the right of the elliptical grid marker. This marker was originally a circle with a diameter equal to the plate thickness which is about half the width of the weld. Normally this circle is centered in both directions of the gage section but in this case is only centered on the axial centerline and at a different axial position on opposite faces. The first crack to penetrate the opposite surface, Fig. 1b, is the middle crack on the left side of Fig. 1a which is about mid-length of the gage section.

An inspection of all photographs indicates that the cracks initiate at the heat effected zone and grow across the width in a direction perpendicular to that of the maximum principal stress and to that of the axial weld. The cracks have a regular spacing in the axial direction since the crack relieves the stress for an axial distance which is a function of the creep strain. The axial extent of the cracking is indicated on the curves in Fig. 3; the higher the peak strain the greater is the extent.

The surface length of the first crack, identified above, is plotted in Fig. 4 as a function of time, the scale for crack length is on the right ordinate. This crack grew primarily in the base metal at nearly a constant rate similar to the overall creep rate. The creep rate and the crack growth rate increased rapidly when this crack reached a length of about 1.8 mm.

5. Discussion of Results

Under constant load the damage mechanism proposed for this composite model is an exhaustion of ductility which will be different for the various zones. The author has shown that this ductility is also a function of the strain rate and the state of stress [3-5]. For the relatively low strain rate of the creep test described here, it is proposed that the creep strain is higher in the grain boundaries and damage is accumulated fastest at grain boundaries orientated nearly perpendicular to the direction of the maximum principal stress. The accumulation of voids or separation of grain boundaries relieves the local strain field.

The grain boundary separation and the adjacent grains form a "cell" and additional voids are impeded for a distance of several grains. With continued creep strain adjacent cells link up in the direction perpendicular to that of the maximum stress to form a crack. Figure 1a illustrates that the cracks at the heat affected zones (HAZ) follow a similar process. The initial crack formed when the local strain at the HAZ near mid-length reached a strain limit of about 4%. With continued creep strain this magnitude of strain spread along the length and additional cracks formed at regular intervals. The extent of cracking shown in Fig. 3 illustrates this strain limit mechanism.

The overall creep rate remained constant during the crack initiation and cracking pattern formation. The crack growth rate into the weld metal was much slower than that in the base metal, Fig. 4, and the more ductile weld impeded the linking of cracks on its opposite sides. However, when the cracks grew to a critical length they began to interact as the net section stress increased. This caused an increase in overall creep rate and a more rapid crack growth rate. Figure 3 shows that the cracking pattern continued to grow after the instability, since the creep continued to spread along the gage length.

The crack growth rate and the overall strain rate are substantially constant after the cracks have been initiated after about 25% of life and up to 70% of life, Fig. 4. Thus the crack growth rate is not a function of the crack length or stress intensity at the crack tip but is controlled by the crack opening displacement which can be considered proportional to the creep of the remaining section beyond the crack. Since the net section stress increases less than 4% for the crack length at 70% of life, the creep rate increased is insignificant. However, when the cracks on opposite sides of the weld begin to interact, the effective crack length approaches nearly twice that on one side and the stress intensity at the crack tip increases rapidly.

The constraints at the heads generate triaxial stress and lower effective stress. The high reinforcement in the width direction causes a lateral stress which is a maximum at the heads and and diminishes toward mid-length of the gage section. The lateral stress increases with increase in axial plastic strain and its effect can be seen in the lateral and axial strain profiles of Figs. 6 and 7 respectively at a creep time of 2886 hours. The average lateral strain at the far end of the fillet near the head is only 0.15% or about 13% of the magnitude of the average axial strain. At the end of the uniform section and at the centerline the average lateral strains are about 1.1 and 2.5% or about 16% or 23% of the magnitude of the average axial strains respectively.

6. Summary

At 593°C the dominate damage mechanism for types 304 and 308 austenitic stainless steels is an exhaustion of ductility. At creep rates below about 10^{-3} percent per hour, cracks initiate in the grain boundaries orientated nearly perpendicular to the maximum tensile stress. For the weldment described here where the base metal, HAZ, and weld metal are strained in parallel, the most vulnerable grain boundaries are shown to be those at the heat affected zones. Cracks initiate at the HAZ when the local permanent strain is about 4%. Because of the increasing strain gradient toward mid-length resulting from the decreasing lateral constraint from the heads of the test specimen, cracks formed at regular spacings at different times at nearly the same strain along the length. The regular spacing is a result of local stress relief due to the opening of the crack. The crack growth is not a function of the crack length or stress intensity at the crack tip but is proportional to the creep deformation in the net section beyond the crack tips which also causes an opening displacement of the crack.

The crack growth rate is about six times faster in the base metal than that across the weld and this is attributed to the higher creep-rupture strength of the weld metal.

7. Acknowledgments

This research was sponsored by the U.S. Energy Research and Development Administration Division of Reactor Research and Development under Contract No. E(11-1)3045. The grid measurements were made by Mr. Edward J. Trax, the creep testing was performed by Mr. Earl H. Vanantwerp and the manuscript was reviewed by Dr. R. L. Johnson. The support and assistance of all parties are gratefully acknowledged.

References

[1] MANJOINE, M. J., "Determination of Plastic or Creep Strains by Grids", ASTM Committee E-28 on Recent Developments in Mechanical Testing, ASTM Annual Meeting, Montreal, Canada, June 1975.

[2] KING, R. T., et al., "Creep Behavior of SMA Type Weld Metal with Controlled Residual Elements", ASME Paper No. 75 WA/PVP-19.

[3] MANJOINE, M. J., "Ductility Indices at Elevated Temperature", Trans. ASME Journal of Engineering Materials and Technology, April 1975, p. 156-161.

[4] MANJOINE, M. J., "Elevated Temperature Mechanics of Metals", 1975 Symposium on Mechanical Behavior of Materials, Society of Materials Science, Japan, Paper D2, 1974.

[5] MANJOINE, M. J., "Basic Creep-Rupture Testing at 1100°F (593°C) of Uniaxially Loaded Specimens of Uniaxially Loaded Specimens of Uniform Sections of Type 304 Stainless Steel", WARD-HT-3045-9 USERDA, TIC, P. O. Box 62, Oak Ridge, TN 37830.

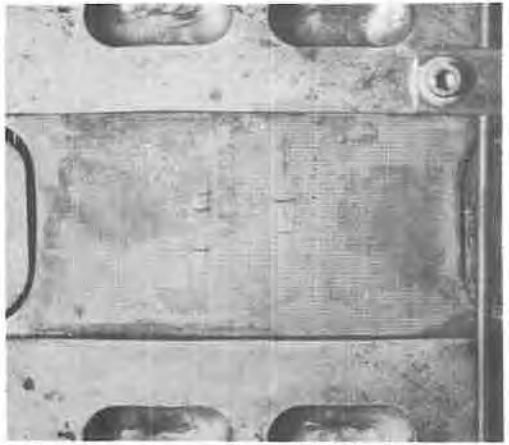

(a) Cracking at Heat Affected Zones

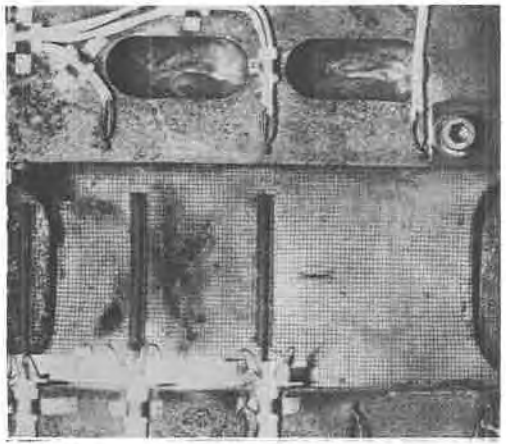

(b) Opposite Side, Instrumentation & Cracking

Fig. 1 - Plate specimen with axial weld after 2886 hours at 23 ksi (159 MPa) and 1100F (593 C)

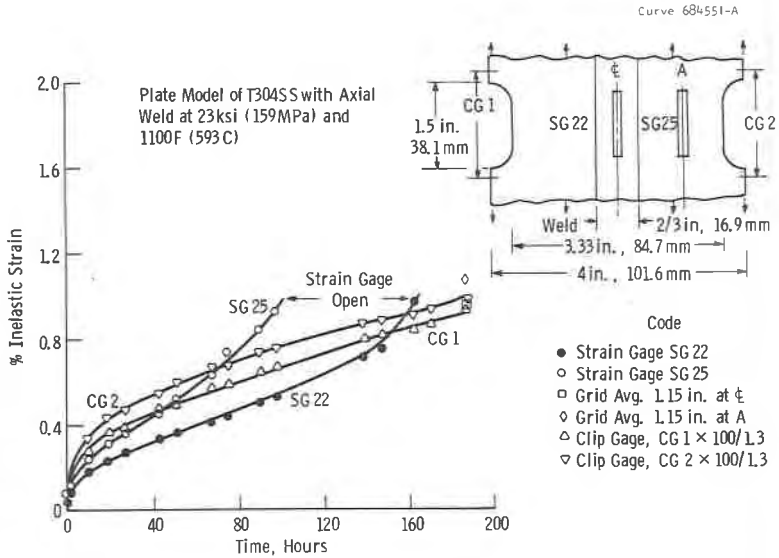

Fig. 2 - Comparison of strain measurements up to 188 hours

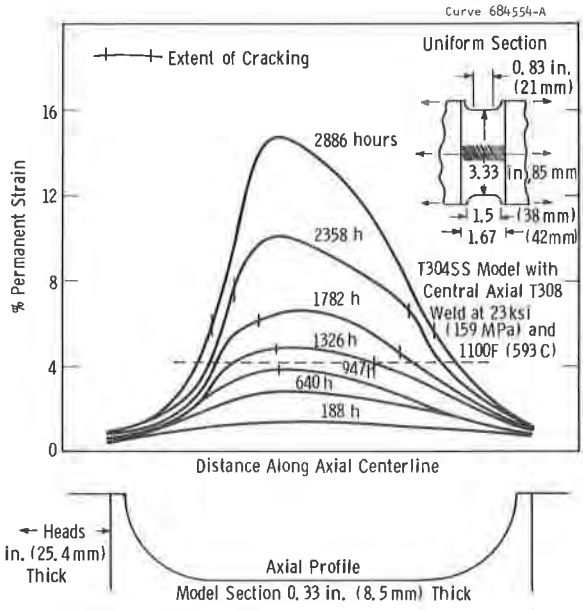

Fig. 3 - Axial strain distributions along centerline of weld from grid measurements

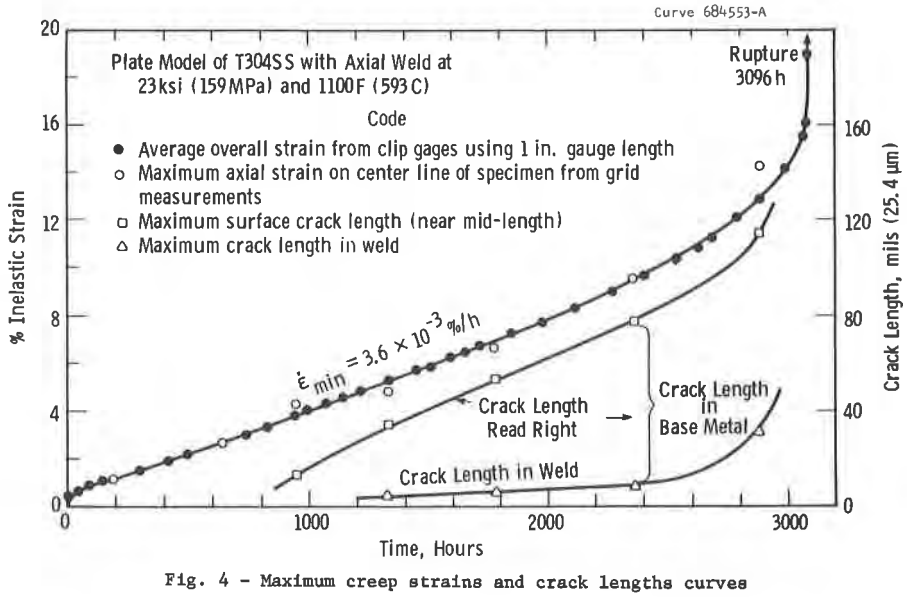

Fig. 4 - Maximum creep strains and crack lengths curves

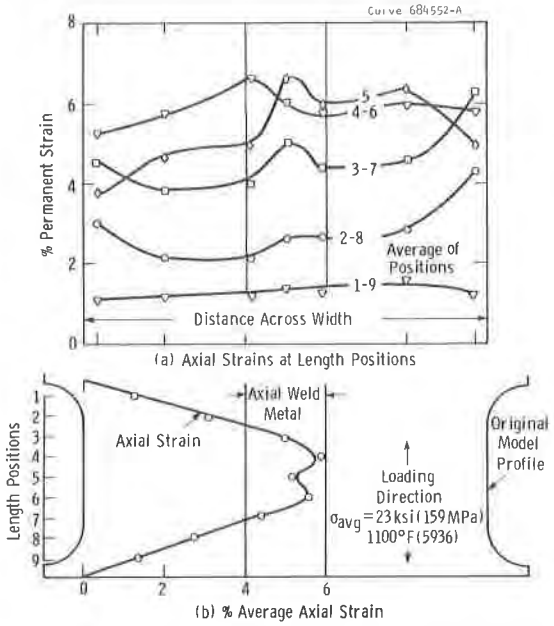

Fig. 5 - Axial strain profiles at 1782 hours from grid measurements

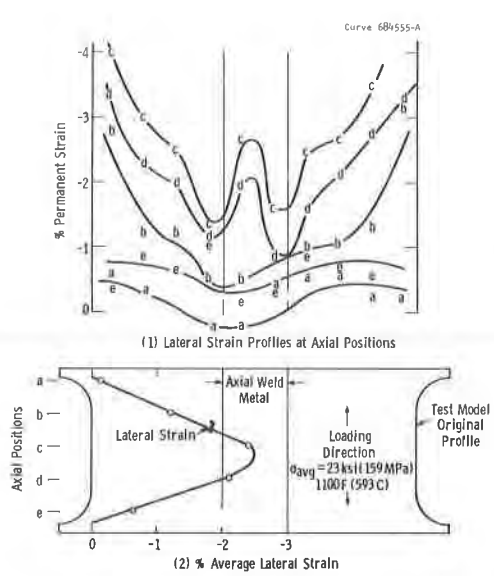

Fig. 6 - Lateral strain profiles at 2886 hours from grid measurements

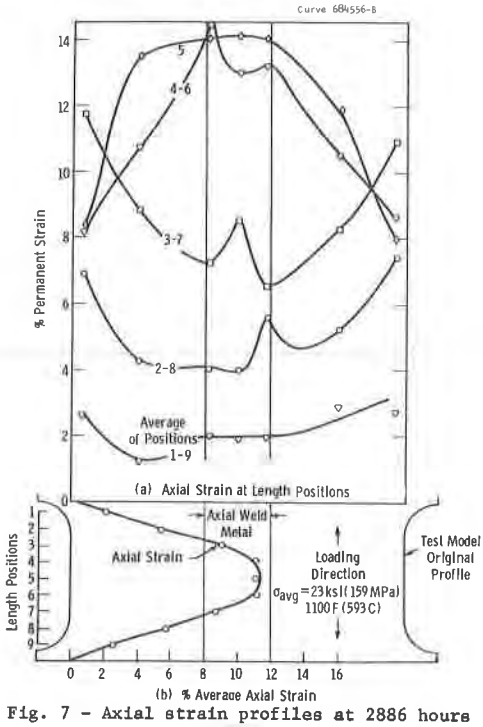

Fig. 7 - Axial strain profiles at 2886 hours from grid measurements